Stirring by Small-Scale Vortices Caused by Patchy Mixing

MILES A. SUNDERMEYER

School for Marine Science and Technology, University of Massachusetts—Dartmouth, New Bedford, Massachusetts

JAMES R. LEDWELL

Department of Applied Ocean Physics and Engineering, Woods Hole Oceanographic Institution, Woods Hole, Massachusetts

NEIL S. OAKEY AND BLAIR J. W. GREENAN

Ocean Sciences Division, Bedford Institute of Oceanography, Dartmouth, Nova Scotia, Canada

(Manuscript received 25 April 2003, in final form 24 September 2004)

ABSTRACT

Evidence is presented that lateral dispersion on scales of 1–10 km in the stratified waters of the continental shelf may be significantly enhanced by stirring by small-scale geostrophic motions caused by patches of mixed fluid adjusting in the aftermath of diapycnal mixing events. Dye-release experiments conducted during the recent Coastal Mixing and Optics (CMO) experiment provide estimates of diapycnal and lateral dispersion. Microstructure observations made during these experiments showed patchy turbulence on vertical scales of 1–10 m and horizontal scales of a few hundred meters to a few kilometers. Momentum scaling and a simple random walk formulation were used to estimate the effective lateral dispersion caused by motions resulting from lateral adjustment following episodic mixing events. It is predicted that lateral dispersion is largest when the scale of mixed patches is on the order of the internal Rossby radius of deformation, which seems to have been the case for CMO. For parameter values relevant to CMO, lower-bound estimates of the effective lateral diffusivity by this mechanism ranged from 0.1 to 1 $m^2 s^{-1}$. Revised estimates after accounting for the possibility of long-lived motions were an order of magnitude larger and ranged from 1 to 10 $m^2 s^{-1}$. The predicted dispersion is large enough to explain the observed lateral dispersion in all four CMO dye-release experiments examined.

1. Introduction

As part of the Coastal Mixing and Optics (CMO) experiment, five dye-release experiments were conducted at middepths over the New England continental shelf to study rates and mechanisms of diapycnal and lateral mixing. The experiments took place over a 3-yr period, 1995–97, all during late summer/early autumn. Concurrent with the 1996 and 1997 dye studies, dissipation rates of temperature variance and turbulent kinetic energy were also measured for the purpose of making direct comparisons of diapycnal diffusivities inferred from these two methods. Results from the dye experiments are described in recent papers by Sundermeyer and Ledwell (2001, henceforth SL), and Ledwell et al. (2004), and in some detail by Sundermeyer (1998). Briefly, analysis of the growth of the patch of tracer in the vertical and horizontal directions indicated that diapycnal diffusivities ranged over $(0.1–1.0) \times 10^{-5}$ $m^2 s^{-1}$ and isopycnal or lateral diffusivities ranged over 0.3–4.9 $m^2 s^{-1}$. Results from the microstructure measurements, including estimates of diapycnal diffusivities, are discussed in a recent paper by Oakey and Greenan (2004).

A major finding of SL is that a significant part of the lateral dispersion observed during CMO could not be explained by vertical shear dispersion or by lateral intrusions of different water masses. In some cases, the observed lateral diffusivities were more than an order of magnitude larger than could be explained by these mechanisms. A similar result was found in a large-scale, open-ocean tracer release experiment by Ledwell et al. (1993, 1998). Specifically, they observed that lateral dispersion on scales of 1–10 km was approximately 40 times that predicted by internal wave shear dispersion.

The results of both of these studies suggest that some other mechanism must have played a significant role in lateral dispersion at scales of 1–10 km. In this paper we

Corresponding author address: Dr. Miles A. Sundermeyer, School for Marine Science and Technology, University of Massachusetts—Dartmouth, 706 S. Rodney French Blvd., New Bedford, MA 02744-1221.
E-mail: msundermeyer@umassd.edu

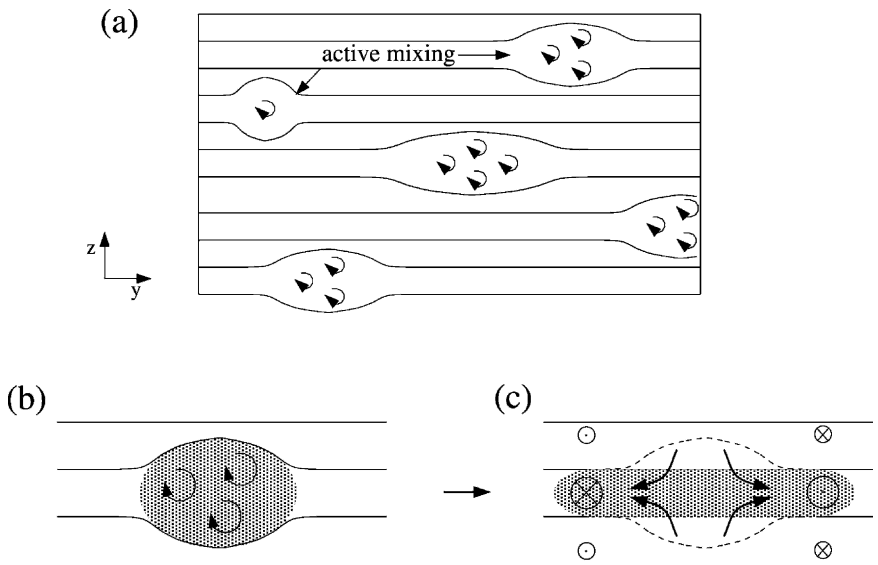

FIG. 1. (a) Schematic of proposed mechanism of lateral dispersion showing mixing that is episodic in space and time. Horizontal lines represent isopycnals, with lenses of well-mixed fluid superimposed. (b) A single mixing event and (c) the ensuing lateral spreading as the stratification adjusts back to its original level. [Reprinted with permission from Sundermeyer and Ledwell (2001), copyright by the American Geophysical Union.]

examine one possibility, stirring by small-scale geostrophic motions caused by patches of mixed fluid adjusting in the aftermath of diapycnal mixing events. The proposed mechanism relies on the fact that vertical mixing in the ocean is not uniform in space and time. Rather, it is episodic, resulting from isolated events due to breaking internal waves (Fig. 1). Motions driven by local baroclinicity associated with mixed patches lead to the horizontal adjustment and thus displacement of regions of well-mixed fluid. The random superposition of these mixing events leads to an effective isopycnal diffusivity.

a. Overview of basic mechanism

The first evidence that turbulence in the oceanic thermocline occurs in intermittent local patches was obtained off the west coast of Vancouver Island by Grant et al. (1968) using temperature and velocity microstructure probes mounted on the bow of a submarine. Their observations showed patches of turbulence ranging from 30 to 170 m in horizontal scale. (Precise vertical scales of patches could not be obtained due to the limited number of probes used.) Such regions of high mixing can be expected to occur as the result of fluctuating vertical shears caused by internal and inertial gravity waves. As envisioned by Phillips (1966) and by Garrett and Munk (1972), local shear instabilities are produced when the shear exceeds a critical value set by a Richardson number criterion. A random superposition of waves causes these instabilities to occur episodically in both space and time. This type of behavior was observed, for example, in the summer thermocline of the Mediterranean Sea by Woods (1968), who used divers to photograph dye streaks during internal wave breaking events.

As a result of episodic mixing, localized regions of reduced stratification are generated preferentially in regions of enhanced mixing, as described in detail by Woods and Wiley (1972) in their discussion of "billow turbulence." Horizontal pressure gradients associated with these stratification anomalies cause the well-mixed regions to move laterally, either geostrophically or not, to form "blini," or pancakes (Phillips 1966; Fig. 1). The types of motions that will occur will depend on the vertical and horizontal scales of the events, and the intensity and duration of the mixing, since these scales ultimately set the scales of the adjustment. If the adjustment time scale is long enough, the motion will become largely geostrophic, and the process is appropriately called geostrophic adjustment; the resulting balanced motions are sometimes referred to as semipermanent finestructure, or the vortical mode (e.g., Kunze 2001). If the time scale is short, rotation is not important and the motion will be mostly a slumping in the direction opposing the pressure gradient; a process we will refer to as "relaxation" since it tends directly toward a barotropic state. If a patch is thin, friction will play an important role in the response from the start and will limit the motion. Regardless of the dominant force balance, we shall use the general term "adjustment" to encompass all of the various motions resulting from the baroclinicity set up by a mixing event.

In all of the above cases, fluid in the weakly stratified patches will move along isopycnals relative to the sur-

rounding fluid. For a single event, the displacement is appropriately described as advective. However, for a large number of events, the cumulative displacements of fluid parcels can be parameterized as an effective lateral diffusivity. How much diffusion will occur will depend on the nature of the adjustment and how long the resultant motions persist. Specifically, we will show that patch scales on the order of the internal deformation radius are optimal for promoting dispersion, since the resultant motions are geostrophically balanced and hence can persist for very long times, and since most of the patch is involved in the motion. In that case, radial displacements associated with the initial stages of adjustment are small compared to those associated with geostrophically balanced flows, and eddy straining dominates the dispersion (e.g., McWilliams 1988; Provenzale 1999). If the adjustment of such events occurs frequently in both space and time, the result may resemble two-dimensional geostrophic turbulence, a topic which has been discussed extensively in the literature (e.g., see reviews by Rhines 1977; McWilliams 1985; Provenzale 1999; and references therein). More generally, however, radial displacements associated with nongeostrophic adjustment may also lead to lateral dispersion, although as will be discussed in section 3b, this will be reduced compared to the geostrophic case.

b. Scope and outline

The formation of localized regions of weak stratification has been well documented in the literature, as noted above (e.g., Phillips 1966; Woods 1968; Woods and Wiley 1972; Garrett and Munk 1972). That well-mixed regions of fluid adjust laterally to form submesoscale geostrophic eddies, or vortical modes, has been firmly established both analytically (e.g., Gill 1981; McWilliams 1988) and in the laboratory (e.g., Griffiths and Hopfinger 1984; Ivey 1987; Thomas and Linden 1996). The implications of patchy diapycnal mixing in the ocean have also been explored (e.g., Vanneste and Haynes 2000; Arneborg 2002). Yet, a simple model linking these processes to lateral dispersion in the ocean is still lacking. The most recent progress in this area comes from a study by Polzin and Ferrari (2004), who examined the effects of blini or vortical motions in the open ocean in the context of the North Atlantic Tracer Release Experiment. Using an empirically derived vortical mode spectrum (Polzin et al. 2003) and theory for two-particle dispersion in two-dimensional turbulence, they showed that vortical mode stirring in the pycnocline of the open ocean can lead to diffusivities of order 1 $m^2 s^{-1}$. In the present study, the effects of vortical motions in the coastal ocean are explored. Specifically, motivated by observations from CMO, we show that the same mechanism can lead to comparable or even greater lateral diffusivities in the coastal ocean. The process we envision here is the same as that discussed by Polzin and Ferrari (2004). However, as we will show, our approach differs somewhat from theirs.

The rest of this paper is organized as follows. In section 2 we review the CMO dye and microstructure data, which together provide the observational basis for this study. The microstructure observations in particular, which were made concurrently with the dye-release experiments, are used to infer approximate spatial and temporal scales of localized diapycnal mixing events. In section 3, we present a simple model for lateral dispersion by small-scale geostrophic motions resulting from the adjustment of mixed patches of fluid. A random walk formulation is used to obtain order of magnitude estimates of the effective lateral diffusivity by this mechanism. A key result is a lower-bound prediction of the effective lateral diffusivity based on the scales of mixed patches and other measurable large-scale parameters. Additional considerations, including the possibility of long-lived vortices and vortex interactions, are also discussed in sections 3 and 4. Specifically, it is shown that the inclusion of these effects may increase our lower-bound estimates by an order of magnitude or more. Section 5 summarizes and concludes.

2. Evidence of small-scale mixing

The CMO dye-release experiments provide estimates of both diapycnal and lateral dispersion (SL; Ledwell et al. 2004). They also provide supporting evidence of the vertical and horizontal scales of mixing. Specifically, as discussed by SL and Sundermeyer (1998), patchiness was observed in the early stages of all of the experiments, particularly the 1996 and 1997 rhodamine dye studies. They found spatial scales in the dye concentrations 6–12 h after injection ranging over 0.5–10 m vertically and a few hundred meters to a few kilometers horizontally. This, combined with the short time it took the dye to evolve from a single coherent streak to a more convoluted/patchy distribution, suggests the presence of shearing and/or straining—that is, stirring at these scales. Some of this stirring, particularly during the initial stages after injection, may have been caused by vortices formed in the wake of the injection sled (e.g., Lin and Pao 1979). However, varying degrees of patchiness superimposed on a background of more diffuse concentrations were also observed later in the experiments.

Velocity and temperature microstructure observations made in concert with the CMO dye-release experiments also showed patchiness at scales of 1–10 m vertically and a few hundred meters to a few kilometers horizontally. These observations, combined with the dye results, suggest that the adjustment of mixed patches of fluid following diapycnal mixing events may have contributed to the observed lateral stirring. The microstructure observations provide the best evidence of the temporal and spatial scales of patchy mixing dur-

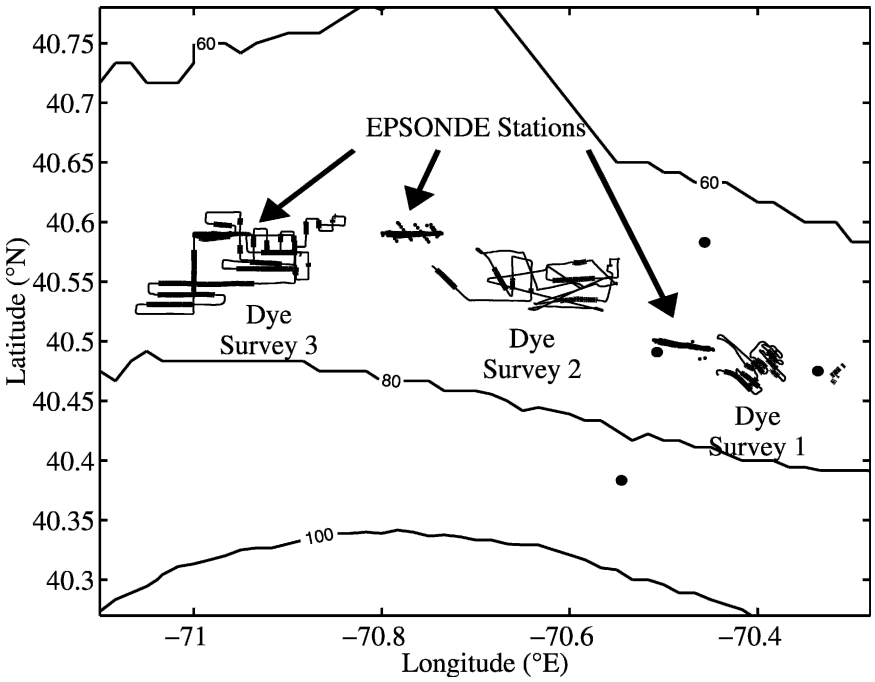

FIG. 2. Ship track during the 1996 fluorescein dye experiment showing the locations of the EPSONDE microstructure stations relative to the three dye surveys. Bold segments in the dye survey tracks indicate where dye was found. Also shown are the 60-, 80-, and 100-m isobaths.

ing the CMO dye studies. The following sections examine these data in some detail.

a. Microstructure patchiness

Velocity and temperature microstructure data were collected during the 1996 and 1997 CMO dye cruises on a schedule of alternating days with the dye surveys for the purpose of making direct comparisons of diapycnal diffusivities inferred from these two methods. We use these data to estimate the time and space scales of patchy mixing. A more complete description of these data can be found in a recent paper by Oakey and Greenan (2004).

The locations of the "EPSONDE" microstructure stations occupied during the 1996 CMO fluorescein dye-release experiment (Experiment 3 in Ledwell et al. 2004) are shown in Fig. 2. For each day that EPSONDE data were collected, a region relatively free of fishing gear was selected as the site of repeated station lines. Each line consisted of a series of profiles taken while the ship was underway at about 1 kt. This provided an effective horizontal resolution of 100–400 m, and an approximate station repeat interval of 2–3 h. For the 1996 fluorescein experiment, 21 EPSONDE lines were occupied, with each line consisting of between 12 and 42 profiles, giving a total of 522 profiles. A comparable number of profiles were taken during the other 1996 and 1997 dye-release experiments.

For each microstructure profile, the dissipation rates of turbulent kinetic energy

$$\epsilon = 7.5 \frac{\mu}{\rho} \overline{\left(\frac{\partial u'}{\partial z} \right)^2} \tag{1}$$

(e.g., Oakey 1988) and temperature variance

$$\chi = 6D \overline{\left(\frac{\partial T'}{\partial z} \right)^2} \tag{2}$$

were computed. Here u' and T' represent the high-frequency velocity and temperature fluctuations, while $\mu/\rho = 1.3 \times 10^{-6}\ \mathrm{m^2\ s^{-1}}$ and $D = 1.4 \times 10^{-7}\ \mathrm{m^2\ s^{-1}}$ are the kinematic viscosity of water and the molecular diffusivity of heat, respectively.

Estimates of ϵ and χ for station line number 40 (occupied 1 day after survey 3 of the 1996 fluorescein dye experiment) and station line number 24 (taken between the first and second survey) are shown in Fig. 3. The data are plotted as a function of potential density, which has been mapped back to a pressure coordinate using the mean density versus pressure relationship for the survey. This was done to remove heaving and stretching of isopycnals caused by internal waves. To distinguish this modified pressure coordinate from the "raw" in situ pressure, we shall refer to the former as "stretched pressure." Also in our analysis, station locations in the horizontal plane were mapped to an advected coordinate system in order to track the ship's motion relative to the water. This was done by integrating the shipboard ADCP data at the depth of the target density surface relative to a common time for each experiment. Henceforth, distances in this new horizontal

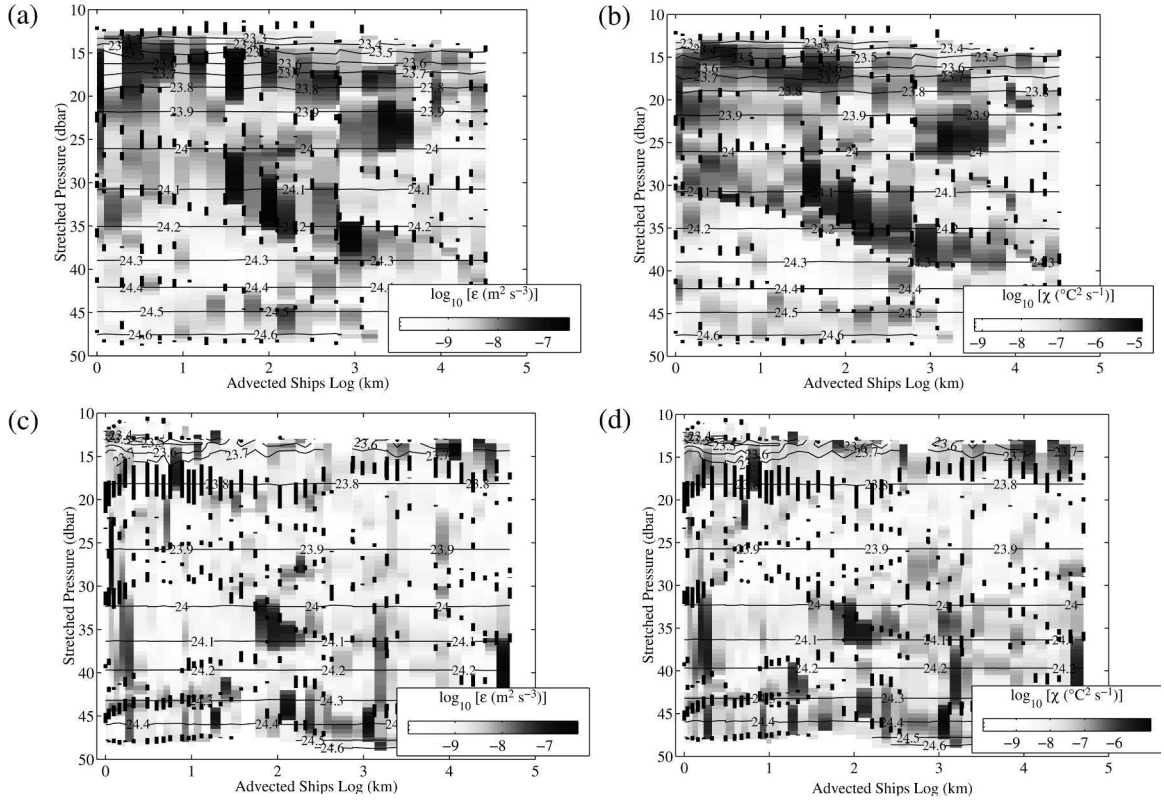

FIG. 3. Dissipation rates ϵ and χ, of (left) turbulent kinetic energy and (right) temperature variance, respectively, for EPSONDE station line numbers (a),(b) 40 and (c),(d) 24, occupied during the 1996 fluorescein dye experiment. Note the localized regions of high velocity and temperature variance as compared with the relatively quiescent background, and in particular the large region of high mixing in (a) and (b) centered at about 30-m depth, which is oblique to surfaces of constant potential density. Thick black line segments in each panel show regions of reduced stratification inferred from density profiles (see also Fig. 7).

coordinate system are termed "advected" distance, that is, "advected ship's log."

Assuming that mixing events occurred where ϵ and χ were more than an order of magnitude greater than their means, the data in Fig. 3 show episodic mixing events on vertical scales of 2–10 m and horizontal scales of a few hundred meters to a few kilometers. Such patches of high dissipation rate were ubiquitous in the microstructure data during the 1996 and 1997 CMO dye experiments. (Microstructure data were not available during the 1995 pilot cruise.) Particularly noteworthy in Figs. 3a and 3b is a layer centered at approximately 35 m, which was oblique to potential density surfaces. As will be discussed in section 4b, this tilt may have affected the ensuing lateral adjustment of the well-mixed fluid. Note that numerous smaller scale events are also visible in both station lines.

b. Time scales and buoyancy flux

Considerable effort has been devoted in the literature to the problem of relating the dissipation rate, ϵ to larger-scale flow characteristics such as shear and stratification (e.g., Henyey et al. 1986; Gregg 1989; Polzin et al. 1995; Alford and Pinkel 2000; MacKinnon and Gregg 2003). The basic premise of such relationships is that the energy dissipated in mixing events is provided by shear in the internal wave field. Scalings, such as the $\epsilon \propto N^2$ relationship derived by Henyey et al. (1986) and the $\epsilon \propto N$ obtained by MacKinnon and Gregg (2003), reflect the fact that internal wave energy, shear, and dissipation all tend to be higher where the mean stratification is greater.

Within a region of given mean stratification, local variations in N might be expected to be negatively correlated with dissipation, because of homogenization of the density profile by mixing. However, the reduction in N caused by diapycnal mixing is determined by the time integral of the buoyancy flux divergence, and not the buoyancy flux itself. For a given mixing event, we might therefore expect N within a mixing patch to vary from some nonzero value at the onset of mixing to some lower value (possibly zero, in the case of complete mixing) by the time the mixing ceases. This will be true regardless of when the maximum value of ϵ and χ occurs. As a result, regions of high ϵ and χ may be accompanied locally by either high or low N.

Nevertheless, an estimate of the amount of work

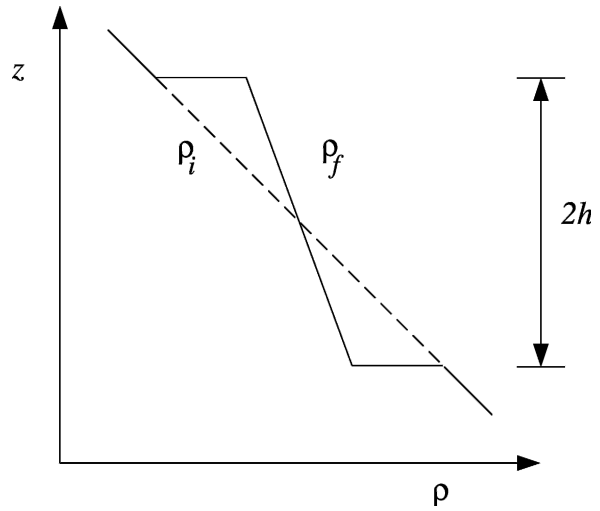

FIG. 4. Schematic of change in stratification and thus PE associated with a single mixing event. The initial density profile, $\rho_i(z)$, is indicated by a dashed line, and the final density profile $\rho_f(z)$, is indicated by a solid line.

done by episodic mixing events can be obtained by examining the dissipation rate and the time scales of the events themselves. Consider in one dimension the case of a single isolated mixing event of half-thickness, h (Fig. 4). For a uniformly stratified water column, the potential energy per unit area can be expressed as

$$\mathrm{PE} = \int_{-h}^{h} \rho g z \, dz = -\frac{2}{3}\rho_o N^2 h^3, \tag{3}$$

where $\rho = \rho_o(1-N^2 z/g)$ is the density, g is acceleration due to gravity, N is the buoyancy frequency, and z is the vertical coordinate. From (3) it follows that the change in PE due to mixing is given by

$$\Delta\mathrm{PE} = \frac{2}{3}\rho_o \Delta N^2 h^3, \tag{4}$$

where $\Delta N^2 = N_i^2 - N_f^2$ is the change in N^2 caused by mixing. Alternatively, the increase in PE due to mixing may be derived by integrating the equation for the turbulent kinetic energy over the volume of the patch and the time of the mixing event, provided buoyancy fluxes through the boundaries of the patch are ignored and the ratio of production of potential energy to dissipation of kinetic energy, Γ, is constant. In that case,

$$\Delta\mathrm{PE} = 2h \int_0^{\Delta t} \epsilon\Gamma\rho_o \, dt = 2h\epsilon\Gamma\rho_o\Delta t, \tag{5}$$

where Δt represents the time over which mixing occurs, and we have assumed for simplicity that ϵ is also constant during the mixing event. Combining (4) and (5), it follows that the change in stratification associated with a patch of mixing is

$$\frac{\Delta N^2}{N^2} = \frac{\Delta\mathrm{PE}}{\mathrm{PE}} = \frac{3\varepsilon\Gamma\Delta t}{N^2 h^2}. \tag{6}$$

Equation (6) suggests that for a given buoyancy frequency N^2 and anomaly height h, we can estimate the change in stratification associated with a dissipation rate ϵ acting for a time Δt. For example, assuming $N = 0.02$ rad s^{-1}, $2h = 5$ m, and $\Gamma = 0.2$, a mixing event with $\epsilon = 10^{-7}$ m^2 s^{-3} lasting for $\Delta t = 1$ h would result in $\Delta N^2/N^2 = 0.1$, or a 10% reduction in stratification. Alternatively, the same ϵ acting for the same period over a vertical scale of $2h = 2$ m would lead to a much greater change in stratification, $\Delta N^2/N^2 = 0.5$, or approximately 50%. Additional estimates of $\Delta N^2/N^2$ for parameter values representative of the CMO dye experiments are listed in Table 1. These results suggest that dissipation rates greater than about 3×10^{-8} m^2 s^{-3} and lasting a few hours or longer can induce significant changes in N^2. This result is most pronounced for mixing events with small vertical scales, that is, $h = 2$ m or less.

Returning to the microstructure data, we now briefly consider the change in stratification induced by diapycnal mixing events. Figure 5 again shows a series of transects of dissipation rate, ϵ, this time in three dimensions. As in Fig. 3, a Lagrangian correction has been applied to each transect using the integrated shipboard ADCP data. However, this time we have used the ADCP data for each depth bin rather than only a single depth corresponding to the target isopycnal surface. Also, here the data are plotted as a function of raw depth rather than stretched pressure. The result is a series of curtain diagrams in a depth-dependent Lagrangian reference frame.

Inspection of Fig. 5 reveals that even with the

TABLE 1. Change in potential energy, $\Delta\mathrm{PE}/\mathrm{PE} = \Delta N^2/N^2$, for select values of dissipation rate ϵ and event time scales Δt. Values representing significant changes in stratification (i.e., $\Delta N^2/N^2 \geq 0.30$) are in italics. Note that by definition, $\Delta N^2/N^2 \leq 1$ so that values greater than or equal to 1 imply complete mixing. That they occur is due to the simplistic but unrealistic assumption that Γ remains constant even as N^2 approaches zero.

	$\Gamma = 0.2$, $N = 0.02$ rad s^{-1}, and $2h = 5$ m			$\Gamma = 0.2$, $N = 0.02$ rad s^{-1}, and $2h = 2$ m		
	$\epsilon = 10^{-8}$ m^2 s^{-3}	$\epsilon = 3 \times 10^{-8}$ m^2 s^{-3}	$\epsilon = 10^{-7}$ m^2 s^{-3}	$\epsilon = 10^{-8}$ m^2 s^{-3}	$\epsilon = 3 \times 10^{-8}$ m^2 s^{-3}	$\epsilon = 10^{-7}$ m^2 s^{-3}
$\Delta t = 1$ h	0.009	0.027	0.086	0.054	0.17	*0.54*
$\Delta t = 2$ h	0.017	0.055	0.17	0.11	*0.34*	*1.1*
$\Delta t = 4$ h	0.035	0.11	*0.35*	0.22	*0.68*	*2.2*
$\Delta t = 6$ h	0.052	0.16	*0.52*	*0.32*	*1.0*	*3.2*

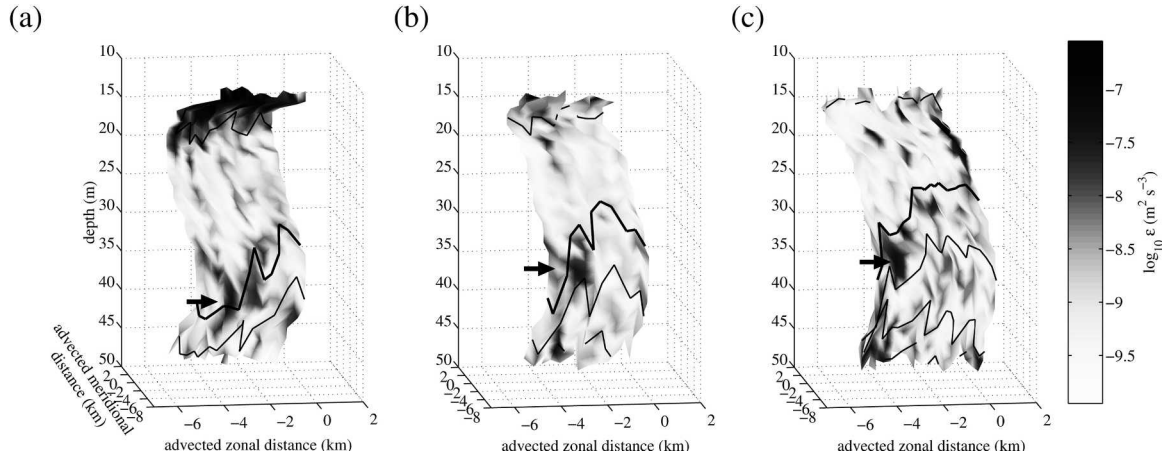

FIG. 5. Dissipation rate, ϵ ($m^2\ s^{-3}$), estimated for three successive transects of the 1996 fluorescein dye-release experiment, [station lines (a) 20, (b) 21, and (c) 22]. Arrows point to a region of high ε, which appears to persist in approximately the same fluid volume throughout the three transects. Isopycnals are also plotted in each panel, with the $\sigma = 24.0$ level plotted in boldface, and incrementing by $\sigma = 0.25$ above and below. Note that the position of the region of high ε relative to the $\sigma = 24.0$ surface is the same in each of the panels. The elapsed time from the beginning of the first transect to the end of the third transect was approximately 4.3 h, suggesting that the mixing persisted for at least that long.

Lagrangian correction, there was significant overlap in the locations of successive EPSONDE station lines. Furthermore, and more interesting, there is visible coherence between the different transect lines. For example, the arrows in Fig. 5 show a region of enhanced dissipation, $\log_{10}(\epsilon) = (-7.5 \text{ to } -7)$, approximately 5 m thick, which persists in approximately the same fluid volume throughout the three transects, a period of at least 4.3 h (the time from the middle of the first to the middle of the third transect). Based on (6), we estimate an event of this magnitude and duration would reduce the stratification by approximately $\Delta N^2/N^2 = 0.1$–0.4, or 10%–40%. This result demonstrates that although we may not be able to directly correlate regions of high ϵ with regions of reduced N^2, as discussed above, some mixing events were sufficiently energetic and long lived to cause order-1 changes in the stratification. Note that several smaller events are also visible in the transects shown in Fig. 5; however, their coherence was not nearly as pronounced. Also, estimates of the Ozmidov scale, $L_O = 2\pi(\varepsilon/N^3)^{1/2}$ from EPSONDE profiles during experiment 3 ranged over 0.2–5 m, suggesting that this was the maximum scale of turbulent eddies in areas of enhanced dissipation. The latter implies that mixing within the large patch shown in Fig. 5 occurred at scales smaller than the observed patch scale—that is, that the patch was a collection of smaller overturns. A similar result showing patch scales many times the overturning scale was obtained by Smyth et al. (2001) based on numerical simulations of Kelvin–Helmholz billows and oceanic microstructure observations. An analogous result, although to a lesser extent, was also found by Alford and Pinkel (2000), who focused primarily on overturning regions with maximum overturning displacements greater than 2 m.

c. Stratification anomalies

We have shown that in some cases mixing events were sufficiently energetic and long lived to cause order one changes in stratification. However, we have also argued that regions of high ϵ and χ, and low N^2 may not necessarily be correlated. Indeed, our attempts to formally obtain such a correlation using the CMO microstructure data were unsuccessful. Nevertheless, distinct patches of reduced stratification were observed in both the tow-yo and microstructure data.

An example of such patches evident in density profiles from a transect occupied during the 1996 fluorescein dye study is plotted in Fig. 6. The profiles were all below the main pycnocline, between about 30–60-m depth. The stratification anomalies, which we define as regions where N^2 was reduced by more than 30% relative to smoothed versions of the same density profiles, ranged in scale from 1 to 10 m thick vertically and a few hundred meters to a few kilometers horizontally. Although larger-scale events are more readily apparent to the eye since they span many profiles, events that span only a few profiles are also evident. Also, in a number of cases anomalies were oblique to potential density surfaces, and were similar in both scale and angle of inclination to the layer seen in Figs. 3a and 3b. Similar stratification anomalies were observed in the other CMO dye-release experiments.

Density profiles obtained from EPSONDE microstructure measurements also showed stratification anomalies. Figure 7 shows an example of this from station line number 40, the same station line shown in Figs. 3a and 3b, except here the data have been smoothed to yield approximately the same resolution as the tow-yo data in Fig. 6. Again localized regions of low stratifica-

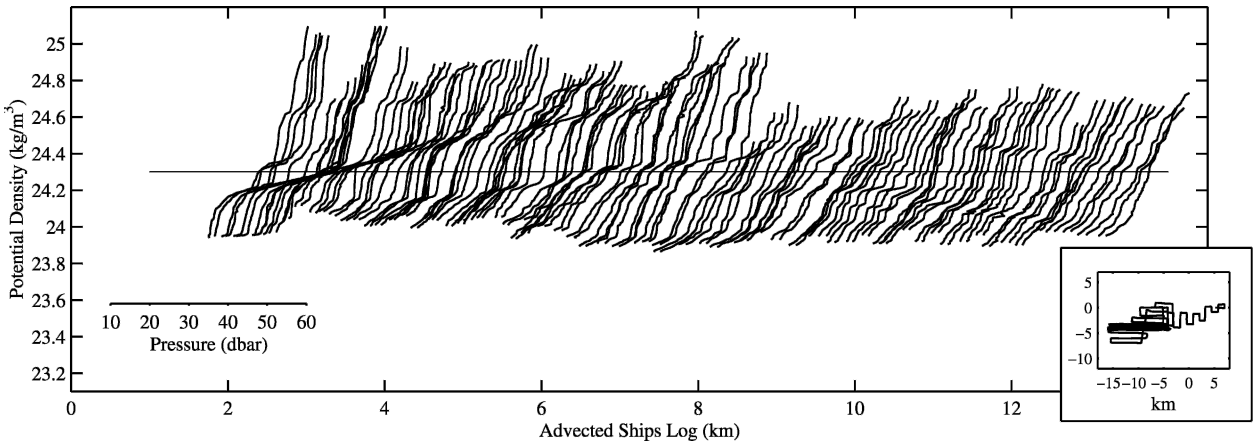

FIG. 6. Density profiles along a transect occupied during survey 3 of the 1996 fluorescein dye experiment showing localized regions of nearly constant density, i.e., low stratification. Pressure is plotted on the x axis and potential density on the y axis so that regions of low stratification appear as horizontal segments of the profiles. Successive profiles are offset by distance along the ship track in an advected coordinate frame. The horizontal line at $\sigma = 24.3$ indicates the density of the dye injection. A plan view of the ship track showing the relative location of this transect (thick line) is shown in the inset to the figure.

tion are evident throughout the water column, particularly below the main pycnocline, which in this experiment was at about 20-m depth.

The observed layers of reduced stratification are similar to those reported by Thorpe et al. (1999) in relatively uniformly stratified waters below the seasonal thermocline of Lake Geneva. Thorpe (1999) described how such layers may be generated through localized mixing associated with internal wave groups, and how the geometry of the layers should relate to the geometry of breaking regions and the propagation characteristics of the waves. Localized mixing is not the only possible explanation for the existence of these regions, however; for example, they may be the result of internal wave strain. Unfortunately, our data do not allow us to discern between these two possibilities.

To assess whether the observed patches of reduced stratification could in fact have been the result of localized mixing, the stratification anomalies indicated in Fig. 7 by boldface line segments are also plotted over the ϵ and χ transects shown in Figs. 3a and 3b. The same analysis was done for station line number 20, shown in Figs. 3c and 3d. As anticipated based on the discussion of the previous section, the correspondence between regions of reduced stratification and high ϵ and χ is sporadic. However, distinct similarities are also apparent, although more so in Figs. 3a and 3b than in Figs. 3c and 3d. For example, in Figs. 3a and 3b, the layer of high ϵ and χ centered at about 35 m coincides approximately with layers of reduced stratification. Rather than being aligned with the region of highest ϵ or χ, however, the low stratification occurs near the boundaries of this region. The reason for this offset is unclear. Nevertheless, this example suggests that these layers are linked. We reiterate, however, that on the scales of interest here, localized regions of low N^2 would be the end product of turbulence and would not necessarily be coincident with regions of high dissipation.

3. A simple analytical model

Results from the CMO dye-release experiments showed patchiness on scales of 1–10 m vertically and a few hundred meters to a few kilometers horizontally. Measurements of the dissipation rate of turbulent kinetic energy ϵ and temperature variance χ also showed event-like mixing at similar scales. Last, tow-yo transects from the dye surveys showed regions of re-

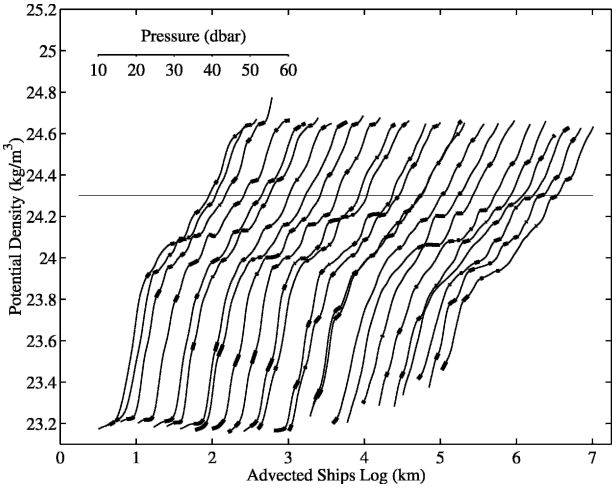

FIG. 7. Similar to Fig. 6, but for EPSONDE station line number 40 occupied 1 day after the third survey of the 1996 fluorescein dye experiment. Boldface line segments indicate regions where N^2 was reduced by more than 30% relative to smoothed versions of the same density profiles.

duced stratification at these same scales. The latter were in some cases related to the regions of enhanced mixing. Together, these observations suggest the presence of episodic mixing and possibly lateral stirring on scales of a few hundred meters to a few kilometers. We now examine whether the adjustment of mixed patches could have led to sufficient lateral stirring to explain the overall lateral diffusivity observed during the CMO dye studies.

a. Momentum scaling

Consider an isolated diapycnal mixing event in which mixing is much greater than the ambient background level. The fate of such an event can be understood as follows. If the timescale of the turbulent mixing event is short compared to the adjustment time of the resulting mixed patch, the process may be thought of as having two distinct phases: a turbulent mixing phase, and an adjustment phase. The mixing phase will create a local buoyancy anomaly. For perfect mixing, the final stratification within this anomaly would be zero so that $\Delta N^2/N^2 = 1$. However, if localized mixing causes an order-1 change in the local buoyancy frequency, but does not lead to perfect mixing, a more realistic value might be, for example, $\Delta N^2/N^2 = 0.5$.

For a given vertical event scale h, we can define a deformation radius associated with the induced stratification anomaly, $R = \Delta N h/f$ (e.g., Gill 1981). Taking a buoyancy frequency, $N = 10$ cph (0.0175 rad s^{-1}), and a vertical event scale of $2h = 5$ m, as were typical for the CMO dye studies, and letting $\Delta N^2 = 0.5N^2$, we find $R = 325$ m. If we assume for the moment that friction is not important during the adjustment of a mixed patch, then for a patch of horizontal scale $2L = 1.0$ km (again typical for CMO) both relative acceleration and Coriolis acceleration will play a role in the adjustment, since in that case the horizontal scale is comparable to the deformation scale.

Using the above assumptions, we can employ simple scaling arguments to understand how the adjustment of mixed patches ultimately leads to an effective horizontal dispersion. Consider the x component of the horizontal momentum equation,

$$\frac{\partial u}{\partial t} + u \cdot \nabla u - fv = -\frac{1}{\rho}\frac{\partial P}{\partial x} + \nu_B \frac{\partial^2 u}{\partial z^2}, \qquad (7)$$

where ν_B represents a background viscosity that may or may not be directly related to the mixing events. This equation can be scaled as follows:

$$\left(\frac{U}{T}\right)\left(\frac{U^2}{L}\right)(fU)\left(\frac{h^2}{\mathrm{L}}\Delta N^2\right)\left(\nu_B \frac{U}{h^2}\right), \qquad (8)$$

where U, L, and T represent velocity, length, and time scales, respectively, and the scaling for the pressure gradient term derives from the hydrostatic equation,

$$\frac{\partial P}{\partial z} = -\rho g. \qquad (9)$$

Equation (7) represents the basic momentum balance associated with the adjustment of mixed patches of fluid. For a single event with $L \geq R$, we envision a classic Rossby adjustment problem. The buoyancy anomaly induced by diapycnal mixing results in a horizontal pressure gradient as represented by the first term on the right-hand side of (7). If the anomaly is axisymmetric, and if the influence of friction is small, this pressure gradient will lead to an initial radial spreading of the well-mixed fluid over a distance of order R (e.g., Fig. 1). As this initial adjustment occurs, a geostrophic flow will be established in the azimuthal direction such that the mixed region rotates anticyclonically. The spreading, and thus a decrease in the PE of the well-mixed fluid, occurs as some of the available potential energy is converted to kinetic energy. There is also a radiation of energy away from the site by internal waves. However, these need not be considered here since their contribution to lateral dispersion is small and since they do not interact significantly with the balanced geostrophic motions (e.g., Reznik et al. 2001).

Whether the radial displacements directed down pressure gradient, or the azimuthal displacements associated with the geostrophic flow are larger, will depend on the scale of the mixed patch. For example, if $L \gg R$, the azimuthal displacements will be much greater than the slumping displacements. Alternatively, if the effects of rotation are small ($L \ll R$), azimuthal displacements will be negligible and the largest displacements will be due to the slumping motions. As will be discussed in section 3c, the greatest net displacement of fluid and hence the largest effective lateral dispersion is expected to occur for $L \sim R$—that is, in a regime where the flow is ultimately geostrophic and the whole patch becomes involved in the adjustment.

b. Vertical diffusion and event time scales

The above considerations can be used to formulate a simple parameterization of the effective horizontal dispersion caused by a collection of random mixing events. However, before we proceed, it is useful to consider how the vertical scales of episodic mixing events are related to the mean vertical diffusion. (We return to the effective lateral dispersion due to episodic mixing events in the next section.)

As suggested by Garrett and Munk (1972), and following section 2b, the mean vertical diffusivity κ_z in a stratified fluid can be related to the scales of episodic mixing events and their frequency of occurrence using PE arguments. Consider a single isolated mixing event of half thickness h, as sketched in Fig. 4. If $Q(h)dh$ represents the expected number of events of half-height between $h \pm \frac{1}{2}dh$ per unit time, per unit depth, then from (3) it follows that the average rate of change in PE density—that is, the buoyancy flux—can be written as

TABLE 2. Event recurrence time scales, $1/\phi$, inferred from (14) for a range of vertical diffusivities κ_z and vertical scales h.

	$2h = 2$ m	$2h = 5$ m	$2h = 10$ m
$\kappa_z = 0.1 \times 10^{-5}$ m^2 s^{-1}	$1/\phi = 2$ days	$1/\phi = 12$ days	$1/\phi = 48$ days
$\kappa_z = 1.0 \times 10^{-5}$ m^2 s^{-1}	$1/\phi = 0.2$ days	$1/\phi = 1.2$ days	$1/\phi = 4.8$ days

$$\int \Delta \mathrm{PE} Q(h)\, dh = \frac{2}{3} \int \rho_o \Delta N^2 h^3 Q(h)\, dh. \qquad (10)$$

Alternatively, writing the buoyancy flux as a diffusivity, κ_z, times a buoyancy gradient,

$$\int \Delta \mathrm{PE} Q(h)\, dh = -\kappa_z \frac{\partial(\rho g)}{\partial z} = \kappa_z N^2 \rho_o. \qquad (11)$$

Combining (10) and (11), the vertical diffusivity can be expressed as the sum of isolated mixing events,

$$\kappa_z = \frac{2}{3} \int \frac{\Delta N^2}{N^2} h^3 Q(h)\, dh. \qquad (12)$$

Recent work by Vanneste and Haynes (2000) suggests this result is valid to within an order-1 coefficient that depends on the probability distribution of the mixing events. (Note, however, that our notation differs slightly from theirs in that we define the frequency of events per unit depth, not over the full water column. Meanwhile our event frequency, ϕ, defined below, is for a given location in the water column, not per unit depth.)

Equation (12) provides a simple relation between the effective vertical diffusivity κ_z, the average frequency of mixing events of a given scale $Q(h)dh$, and the buoyancy anomaly associated with these events ΔN^2. For simplicity, let us assume that all events have the same half-thickness, h, and buoyancy anomaly, ΔN^2. Then (12) reduces to

$$\kappa_z = \frac{1}{3} \frac{\Delta N^2}{N^2} h^2 \phi, \qquad (13)$$

where ϕ represents the average frequency of events. In the present context, (13) is most useful if the vertical diffusivity is known, as from the dye experiments or microstructure. In this case the frequency of events, ϕ, can be estimated from observations of the vertical scale h and the buoyancy anomaly ΔN^2; that is,

$$\phi = 3 \frac{N^2}{\Delta N^2} \frac{1}{h^2} \kappa_z. \qquad (14)$$

Equations (13) and (14) show that for a given vertical diffusivity, κ_z, the larger the thickness of the mixing events, the less frequently they must occur. For example, for the second of the 1996 CMO dye experiments, the vertical diffusivity in the lower part of the patch was $\kappa_z = 0.9 \times 10^{-5}$ m^2 s^{-1}. Assuming a typical buoyancy anomaly, $\Delta N^2 = N^2$ and a typical vertical scale, $2h = 2$ m, (14) implies an average event recurrence time of $1/\phi = 0.2$ days. Alternatively, mixing events of vertical scale $2h = 5$ m would result in a larger event recurrence time, $1/\phi = 0.3$ days. Similar calculations for a variety of combinations of patch thicknesses and vertical diffusivities are listed in Table 2. For a reasonable range of vertical scales h and vertical diffusivities κ_z, the inferred event recurrence times range from $1/\phi = 0.2$ days to $1/\phi = 48$ days.

Relevant to this range of recurrence times, is that according to (13) and (14), ϕ also depends on $\Delta N^2/N^2$, which we assumed here has a nominal value of 0.5. All else being equal, however, (6) suggests that $\Delta N^2/N^2$ may itself vary, so that the actual range of recurrence times may not be as wide spread as Table 2 suggests. Alternatively, however, if ϵ, Δt, and h are not independent—for example, if the vertical scale of the mixed patches is related to the dissipation rate through the Ozmidov scale, $L_O = 2\pi(\varepsilon/N^3)^{1/2}$ (e.g., Smyth et al. 2001)—then (6) implies that any such reduction in the range of recurrence time scales may be negated. Regardless of the actual value of $\Delta N^2/N^2$, however, the important points in Table 2 are 1) to show approximately how the event recurrence time scale varies for different vertical scales, and 2) to show that for the same vertical patch scale h, the recurrence time scale is always less than the frictional time scale, as we shall now explain.

The frictional time scale, h^2/ν_B associated with vertical viscosity is also important to the adjustment of diapycnal mixing events. Here we imagine that diapycnal mixing events and their resultant stratification anomalies occur and relax amidst some background vertical viscosity, ν_B, which may be molecular viscosity or may represent processes acting on small scales at times outside of the mixing events. For purely molecular viscosity acting on a very thin layer, the horizontal pressure gradients associated with a density anomaly may be balanced by friction, and a frictional adjustment may occur. In the case of an eddy viscosity, we might imagine that as small-scale eddies redistribute momentum, they would also mix away the density anomaly associated with the mixing event, halting the adjustment. Although it is conceivable that internal waves can transfer momentum vertically independent of turbulent mixing events, thus enhancing ν_B somewhat, we shall assume that $\nu_B \leq \kappa_z$—that is, the background viscosity is less than the diffusivity due to mixing events. Oakey and Greenan (2004) estimated eddy viscosities during CMO from 4×10^{-5} to 1×10^{-4}, averaged over regions of both high and low ε. However, if event-like mixing dominated over background mixing, which we believe

to have been the case, the background viscosity would have been much less than this and hence may still have been less than or of the same order as the total vertical diffusivity. In either case, a short frictional time scale would limit the amount of time that diapycnally mixed fluid would have to be displaced laterally during adjustment.

Whether friction is likely to affect the adjustment of mixed layers can be determined. Table 3 lists the frictional time scales, h^2/ν_B for molecular and modest eddy viscosities over a range of vertical event scales typical of CMO. As the resulting times are generally of order a day or more, viscous accelerations are unlikely to have been important relative to the Coriolis acceleration for these events. Furthermore, for $\nu_B = \kappa_z$, (and especially for $\nu_B < \kappa_z$) and comparable vertical scales h, the inferred frictional time scale, $T\nu_B = h^2/\nu_B$ is always larger than the recurrence time scale, $1/\phi$. Note that this is true independent of the value of $\Delta N^2/N^2$. This follows directly from (14) and the definition of the frictional time scale; that is,

$$\frac{T_{\nu_B}}{1/\phi} = \left(\frac{h^2}{\nu_B}\right)\left(3\frac{N^2}{\Delta N^2}\frac{\kappa_z}{h^2}\right) = 3\frac{N^2}{\Delta N^2}\frac{\kappa_z}{\nu_B} \geq 1, \quad (15)$$

since by definition, $\Delta N^2/N^2 \geq 1$ and by assumption $\nu_B \leq \kappa_z$. This suggests that successive anomalies will likely overlap with their predecessors. In an extreme case, if a density anomaly is completely mixed away by a new event, the recurrence of events will thus halt (or at least significantly modify) the adjustment of previous events long before friction can play a significant role.

c. Effective lateral dispersion

The size of the deformation radius estimated in section 3a and the time scales estimated in section 3b are all consistent with the idea that episodic mixing events observed during the CMO dye-release experiments may have resulted in the geostrophic adjustment of mixed regions. We now consider the effective lateral diffusivity associated with a collection of such events. First, we consider dispersion by a field of independent adjustment events, that is, assuming that vortices do not interact. We then consider how the interaction of vortices might modify our results.

Suppose that patches of diapycnal mixing occur on horizontal scales comparable to or greater than the deformation radius, and that the recurrence time scale of events, $1/\phi$ is greater than or equal to the rotation time scale, $1/f$ so that events adjust under the influence of rotation before being disturbed by subsequent events. In this case, after sufficient time has elapsed, the dominant balance in the horizontal momentum Eq. (7) will ultimately be between the pressure gradient and Coriolis acceleration. The horizontal velocity associated with the adjustment of a mixed patch thus scales as

$$U \sim \frac{h^2\Delta N^2}{Lf}. \quad (16)$$

TABLE 3. Viscous time scales, h^2/ν_B, showing the time it would take for the motion of an anomaly of a given vertical scale h to be arrested by viscous forces.

	$2h$ = 2 m	$2h$ = 5 m	$2h$ = 10 m
$\nu_B = 0.1 \times 10^{-5}$ m^2 s^{-1} (molecular viscosity)	12 days	72 days	289 days
$\nu_B = 1.0 \times 10^{-5}$ m^2 s^{-1} (eddy viscosity)	1.2 days	7.2 days	29 days

Now consider the effect of many such events on the dispersal of a passive tracer. The effective horizontal diffusivity associated with the events can be thought of as a random walk of fluid parcels with horizontal step size S and frequency Φ—that is, $\kappa_H \sim \frac{1}{2}S^2\Phi$. In the case of geostrophic adjustment, the step size S is at least of order the geostrophic velocity (16) times the adjustment time scale $T \sim 1/f$. An alternative choice of time scale for this purpose is the eddy turnover time. However, for Rossby number $R^2 \leq 1$, which we assume to be the case here, the eddy turnover time is greater than or equal to an inertial period, so that $1/f$ gives a lower bound on the displacement; that is,

$$S \sim UT \sim \frac{h^2\Delta N^2}{Lf^2} = \frac{R^2}{L}. \quad (17)$$

Meanwhile, in the simplest case, the frequency of taking a step is given by the frequency of the diapycnal mixing events themselves. Thus, the effective horizontal diffusivity is

$$\kappa_H \approx \left(\frac{1}{2}\right)S^2\Phi \sim \left(\frac{1}{2}\right)\frac{h^4\Delta N^4}{L^2f^4}\phi, \quad (18)$$

or, substituting for $\Delta N^2h^2\phi$ in terms of $N^2\kappa_z$ from (14), and for the deformation radius, $R = \Delta Nh/f$,

$$\kappa_H \sim \left(\frac{3}{2}\right)\left(\frac{N^2}{f^2}\right)\left(\frac{R^2}{L^2}\right)\kappa_z. \quad (19)$$

Equations (18) and (19) provide an estimate of dispersion by vortices generated through the adjustment of mixed patches. However, this estimate is conservative for at least two reasons. First, we used $1/f$ rather than the (larger) eddy turnover time to estimate the step size S. Second, if motions are long lived, they may interact, enhancing the dispersion more than (18) and (19) imply.

Consider a single geostrophic vortex generated by the adjustment of a mixed patch of fluid. If the vortex is long lived, the displacement or step size experienced by a fluid parcel within the vortex will increase until it completes half of a revolution around the vortex, or about one-half of an eddy turnover time. Assuming an axisymmetric Gaussian-shaped vortex (e.g., McWil-

liams 1988), a parcel 1 deformation radius from the vortex center will take 1–2 inertial periods to do this. Meanwhile, at distances greater than a deformation radius, but still within the influence of the vortex, parcels will take longer to achieve the same angular displacement. As a result, even after many inertial periods, some parcels will not have completed even one-half of a revolution. Once they do, however, their corresponding linear displacements will be greater than parcels nearer to the vortex center. The rms displacement of all fluid parcels combined will thus continue to grow for multiple eddy turnover times, that is, several inertial periods. Eventually the rms displacement will asymptotically approach a finite value (e.g., Rhines and Young 1983). Using a simple analytical/numerical model for an idealized inviscid Gaussian vortex, we have found the rms displacement of fluid parcels to grow linearly for small times, asymptotically approaching a fixed value for very large times (i.e., many tens of inertial periods), with a transition period in between. For the size and strength of the vortices envisioned here, we thus find that the mean squared displacement of parcels within a few deformation radii from the vortex center may be as much as 5–10 times as large as (18) suggests.

A second means by which long-lived vortices can lead to an increased dispersion is by interacting nonlinearly. In that case, the implicit assumption that closed streamlines will limit vortices' ability to disperse fluid, breaks down. Instead, vortices will mutually advect, as well as merge and/or destroy one another, and the mixing becomes similar to two-dimensional turbulence. Pasquero et al. (2001) and Pasquero et al. (2002) found that in this realm, Lagrangian decorrelation time scales range from 4–18 times the eddy turnover time.

In the case of interacting vortices, and possibly also in the case of isolated vortices but before the mixing is complete within closed streamlines, the viscous time scale $T\nu_B$ or, nondimensionally, the Ekman number (fh^2/ν_B) provides a measure of the time that a given vortex will contribute to lateral dispersion. For interacting vortices, in analogy with two-dimensional turbulence, this can be seen by combining simple energetics arguments with Taylor's (1921) eddy diffusion formulation, $\kappa_H \approx T_I\mathrm{KE}$, where KE is the kinetic energy of the turbulent flow field, and T_I is the integral time scale of the motion. Assuming the KE of the eddy field is given by a balance between the production of eddies by the adjustment of mixed patches and their decay by viscous forces, the diffusivity can be expressed as

$$\kappa_H \approx T_I\,\mathrm{KE} \approx T_I \times (\text{Production rate of KE})\left(\frac{h^2}{\nu_B}\right). \tag{20}$$

Let the production rate of KE be given by the frequency of mixing events ϕ times some fraction of the PE generated by individual events per (3); that is,

$$\text{Production rate of KE} \sim \phi \times \left(\frac{2}{3}\rho_o \Delta N^2 h^2\right), \tag{21}$$

where the rhs has now been normalized by h to obtain KE per unit volume. Assuming that the integral time scale T_I is approximately equal to the eddy turnover time—that is, a few inertial periods—and again using (14), it then follows that the horizontal diffusivity for nonlinearly interacting vortices scales as

$$\kappa_H \sim \alpha\left(\frac{N^2}{f^2}\right)\left(\frac{h^2/\nu_B}{1/f}\right)\kappa_z, \tag{22}$$

where α is an unknown coefficient, presumed to be of order 1.

Equation (22) is very similar to (19), the differences being the factor (R^2/L^2) in (19), which we assumed to be of order 1, and the appearance of the Ekman number in (22), which sets the overall strength of the turbulent eddy field. Although these two expressions were derived in much different ways, the process they represent is similar. Still, they represent two extremes for the expected lateral dispersion. Specifically, (19) represents the case in which vortices do not interact and the dispersion is limited to one or two inertial periods, while, (22) assumes that vortices are long-lived and do interact. For the case of the interacting vortices, we presume that the Ekman number is greater than 1. In fact, for CMO, based on Table 3, we believe it was closer to 10. Also, for the case of noninteracting vortices, we have argued above that (19) may still underestimate the dispersion by up to an order of magnitude.

Both of the above scalings provide estimates of the effective horizontal diffusivity due to the adjustment of episodic mixing events when events are of large enough horizontal scale to adjust geostrophically. Furthermore, they both show that the effective horizontal diffusivity by the adjustment of mixed patches of fluid can be written in terms of the vertical diffusivity times a scaling factor, which depends on known and/or measurable parameters.

The above parameterizations are similar to one obtained by Young et al. (1982) for shear dispersion due to internal waves. However, the motions modeled here are entirely isopycnal; we have not yet considered the interaction between vertical shear and vertical diffusion. That process is compared with the present one in the appendix. The diapycnal diffusivity enters both (19) and (22) through the rate of production of vortices, not through a shear dispersion model. In fact, SL showed that shear dispersion by internal waves was insufficient to explain the lateral dispersion observed in CMO.

The diffusivity predicted by (19) and (22) can be compared directly with results of SL from the CMO dye studies. Their "irreversible" lateral diffusivities represent the effective diffusion along isopycnals, excluding "reversible" processes such as oscillatory shears, but including irreversible effects such as small-scale stirring

TABLE 4. Comparison of irreversible lateral diffusivities estimated from the CMO dye-release experiments, and values predicted for vortical mode stirring using (19) and (22).

	1995 (40 m)	1996 (35 m)	1996 (46 m)	1997 (18 m)
N^2 rad s^{-1}	12	5–6	12	13–18
$\kappa_z \times 10^{-5}$ m^2 s^{-1}	0–1.5	1–3	0.2–1.0	0.2
κ_H m^2 s^{-1} (CMO)	4.9 (2.9–7.3)	4.6 (3.0–6.5)	0.5 (0.1–1.1)	0.3 (0.1–0.6)
κ_H m^2 s^{-1} [Eq. (19)]	0–1.1	0.1–0.6	0.1–0.7	0.2–0.3
κ_H m^2 s^{-1} [Eq. (22)]	0–11	1.3–5.5	1.5–7.3	1.7–3.3

along isopycnals and shear dispersion. Using typical values from CMO, $N^2/f^2 \sim (0.1–1) \times 10^5$, and assuming mixing events of horizontal scale of order the deformation radius (R^2/L^2), (19) yields

$$\kappa_H \sim (0.1–1) \times 10^5 \kappa_z, \tag{23}$$

which we have argued is a conservative estimate of the dispersion. Alternatively, assuming a lower-bound estimate of the Ekman number based on a 2-m event and a background viscosity of $\nu_\beta = 10^{-5}$ m^2 s^{-1}, that is, $(fh^2/\nu_B) = 10$, (22) yields

$$\kappa_H \sim (1–10) \times 10^5 \kappa_z. \tag{24}$$

For the range of vertical diffusivities estimated from the CMO dye studies, $\kappa_z = (0.1–1.0) \times 10^{-5}$ m^2 s^{-1}, the above expressions thus give horizontal diffusivities of $\kappa_H \sim (0.1–10)$ m^2 s^{-1}. Comparing these estimates with the values of κ_H estimated during CMO (Table 4), we find that the predicted dispersion spans the range of the observed dye dispersion. Analogous predictions using diapycnal diffusivities estimated from microstructure measurements by Oakey and Greenan (2004) and by MacKinnon and Gregg (2003) give similar results.

4. Discussion

The above scale analysis provides a simple framework for understanding how the adjustment of diapycnal mixing events can lead to an effective lateral dispersion. It leads to simple parameterizations of the induced lateral dispersion in terms of the scales of diapycnal mixing events, the net diapycnal diffusivity they induce, and measurable external parameters. However, there are a number of aspects of the model that warrant further discussion.

a. Random walks and nonlinear interactions

A fundamental issue in the above scaling is the question of how well our assumption of a random walk diffusivity applies to a situation such as CMO in which the duration of the dye experiments is only a little longer than the time between diapycnal mixing events, that is, 3–5-day experiments, in comparison with approximately an inertial period, that is, 18 h. Indeed, if both the event frequency and the frictional time scale (i.e., the lifetime of an individual event) are small, a random walk scaling would not be appropriate. However, if the frictional time scale is long relative to the time between events (i.e., large Ekman number), the number of vortices stirring the tracer at any given time, and hence the effective frequency with which an individual fluid parcel takes a step, may be many times larger than the actual generation frequency of events. In addition, as the dye patch grows, the area of the patch and hence the number of vortices acting on it will grow geometrically, thus increasing the effective number of independent Lagrangian trajectories within the patch. These two factors combined can lead to the diffusive spreading of a dye patch after a surprisingly short time.

Related to the above, an interesting aspect of the random walk scaling given by (19) is that it does not require that vortical motions generated by mixing events interact nonlinearly as a turbulent flow field. In fact, by neglecting the effect of such interactions, (19) implicitly assumes that lateral stirring by vortices can occur even if mixing events are sparse in space and time. In that case, the stirring may look less like turbulence and more like, for example, the "blinking vortex" model of Aref (1983). (In our case, however, a given vortex would "blink" on and remain so for many inertial periods rather than switching on and off in the same location indefinitely.) For CMO at least, we estimated that the recurrence time scale is shorter than the frictional time scale, so that vortices likely do interact. This was taken into account to some degree in our revised scaling given by (22). However, given our uncertainty about the frequency of mixing events and the background viscosity, we cannot say for certain which of these scalings is most appropriate for which experiment, only that they appear to be of the right order of magnitude compared with the observations.

b. The geometry of mixed patches

The scalings given by (19) and (22) are for the idealized case of an axisymmetric vortex, assuming that mixed patches of fluid adjust geostrophically. The size of the deformation radius estimated in section 3a and the time scales estimated in section 3b suggest that, regarding the latter at least, this was indeed the case during CMO. Mixed patches that adjust geostrophically are optimal for generating lateral dispersion because they provide the greatest stirring for a given amount of vertical mixing. Indeed, as discussed by Sundermeyer (1998) it can be shown that if $L = R$, the patches will relax with relatively small displacements. Similarly, if

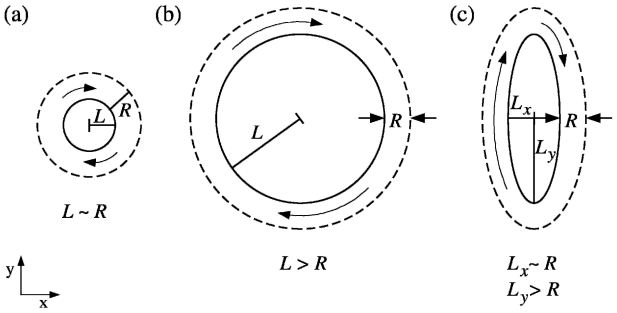

FIG. 8. Schematic of (a) a radially symmetric mixing event of horizontal scale $L \sim R$, (b) a radially symmetric mixing event of scale $L > R$, and (c) an elongated mixing event of mixed scales.

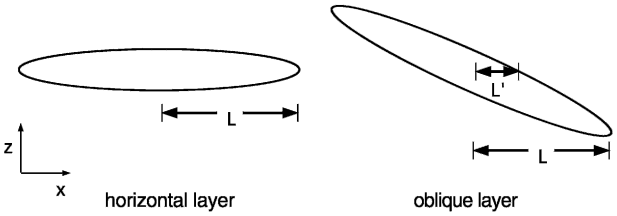

FIG. 9. Schematic of horizontal vs oblique mixed layers showing the difference in effective horizontal scales, $L' \leq L$.

patches are thin in the vertical in the sense that the frequency of mixing events is large when compared with f [e.g., see (14)], but not so thin that friction dominates their initial adjustment, and further, if new events completely interrupt the flow of previous events, then the displacements will again be relatively small. Last, if the mixed patches are thin enough that the frictional time scale is short when compared with $1/f$, then again the resulting displacements will be relatively small.

A second consideration regarding the geometry of mixed patches arises in the more general case when mixing events adjust geostrophically but are not horizontally symmetric; in this case, the dispersion will be further modified. Consider an event which is of order the deformation scale in one horizontal dimension, but much larger in the other. In this case, the mixed region will again adjust geostrophically, spreading laterally while setting up a geostrophic flow. However, instead of a symmetric vortex, the adjusted state will be a long band with geostrophic flow in the direction of the longitudinal axis of the mixed region (Fig. 8c). The displacements associated with this geostrophic flow will be larger than the azimuthal displacements associated with a symmetric patch that is of order of R (Fig. 8a). This is because in the case of an elongated patch of mixed fluid, the geostrophic flows can transport fluid much further than a deformation radius in the direction of the major axis of the mixed region (this assumes again that the geostrophic flows persist longer than the initial adjustment time before being interrupted by a new mixing event or arrested by friction). The case of symmetric mixed regions with $L \gg R$ is similar (Fig. 8b), except that only edges (with width of order R) are set into motion.

A third geometrical consideration for mixed patches of fluid is that, as noted in section 2c, density anomalies observed during the CMO dye studies were frequently oblique rather than parallel to potential density surfaces. The effective horizontal scales of the mixed layers, $L' \leq L$, was therefore reduced relative to the case where layers are not tilted. This is shown schematically in Fig. 9. According to the scaling given by (19), the predicted horizontal diffusivity would thus increase for large tilted layers, since the scale factor $R^2/L'^2 \geq R^2/L^2$. Note, this assumes their effective horizontal scale, L', was still of order R or greater.

Last, relating to our discussion in section 2b, is the question whether the adjustment of patches consisting of multiple overturns can be modeled collectively as a single adjustment event, as we have done; or alternatively, whether individual overturns should be considered individually, each going through its own adjustment, and possibly interacting and merging as a result of the adjustment. Considering (6) and (14), we believe that whether mixed patches are one-half as large with 2 times the change in stratification, or vice versa, has little impact on our final result, since both of these expressions suggest that the more important quantity is the change in PE induced by diapycnal mixing—that is, the net diapycnal diffusivity. Specifically, given the integral constraint that κ_z imposes on the buoyancy flux, it follows from the final scaling for κ_H given by (19) and (22) that any change in the vertical scale of the events h would necessarily be offset by a change in ΔN^2, leaving κ_H relatively unchanged. The one exception is the Ekman number scaling, (fh^2/ν_B) in (22). However, our estimate of this parameter in section 3c is already quite low because of our assumption of a 2-m event scale and a conservative estimate of the eddy viscosity. Furthermore, if smaller events do interact nonlinearly and possibly merge, as discussed in the previous section, then the effective Ekman number may also remain relatively unchanged.

c. Additional considerations

One place where we may have overestimated the dispersion by mixed patches of fluid is in our use of a simplified random walk scaling, $\kappa_H \sim \frac{1}{2}S^2\phi$, which implicitly assumes that S (and hence S^2) and ϕ are uncorrelated. However, if S^2 and ϕ are correlated, then this κ_H may be an underestimate because it neglects the cross-correlation term. Conversely, if S^2 and ϕ are negatively correlated, then by the same reasoning, κ_H may be an overestimate. Indeed, comparing the step size estimated in (17) with the step frequency estimated in (14), and assuming f, L, and κ_z are independent variables, we anticipate that, if anything, S (and hence S^2) and ϕ would be inversely (i.e., negatively) correlated through their dependence on $\Delta N^2 h^2$.

Another factor affecting the dispersion by mixed patches of fluid is that if layers do adjust geostrophically and then subsequently decay by viscous damping, additional spreading of the mixed fluid may occur during the spindown of the geostrophic flow (e.g., Gill 1981). This will again increase the effective lateral diffusivity associated with the relaxation of mixing events compared to (19).

The adjustment of diapycnal mixing events may also contribute to lateral dispersion by vertical shear dispersion. Given the relatively small lateral scale of the events compared to the scale of the dye surveys, it is likely that the relatively low-frequency vertical shears associated with them would have been aliased as high-frequency shears by shipboard ADCP observations and would therefore not be accurately portrayed in the analysis of SL. However, in the appendix, we show that shear dispersion associated with the adjustment of mixed patches is less than the effective dispersion due to purely isopycnal motions. Thus we believe that shear dispersion is only of secondary importance to the process described here.

We have argued that the adjustment of patches created by diapycnal mixing events would manifest itself in the form of small-scale stirring on the same scales at which the diapycnal mixing occurs—that is, 0.5–10 m vertically and a few hundred meters to a few kilometers horizontally. Alternatively, however, within the context of this same mechanism, suppose that vertical mixing during a particular dye experiment was due primarily to one (or very few) large event(s). In the extreme case of a single large mixing event, the dye would mix rapidly in the vertical for a brief time and then not at all. Meanwhile, in the horizontal direction the dye would appear to spread continuously, possibly as a single or very few streaks, as the well-mixed fluid adjusted laterally and ultimately relaxed due to friction. In that case, the horizontal dispersion might more appropriately be described as an advective rather than a diffusive process. However in practical terms, without additional information about the larger-scale flow, this advection may be indistinguishable from other baroclinic and/or barotropic shearing or straining processes.

5. Summary and conclusions

Observations from the CMO dye-release experiments (see also Sundermeyer and Ledwell 2001; Ledwell et al. 2004) and concurrent microstructure observations (see also Oakey and Greenan 2004) are consistent with the view that mixing in the stratified waters of the continental shelf occurs episodically in both space and time. The observations suggest that the scales of mixing ranged over 2–10 m in the vertical and a few hundred meters to a few kilometers in the horizontal. In this paper, we have attempted to show that diapycnal mixing events at these scales can lead to significant lateral stirring through the adjustment of mixed patches of fluid. Scale analysis applied to the horizontal momentum equations along with a simple random walk formulation were used to estimate the effective horizontal diffusivity due to this mechanism. A similar result was also obtained directly from energetics considerations using Taylor's (1921) eddy diffusion theory.

A major result of this study is that there is an optimal scale of mixing events to achieve a maximum effective lateral diffusivity. The basic result, which we believe represents a lower-bound prediction, is given by (19). A more representative prediction, which accounts for the lifetime of vortices and the possibility of vortex interactions, is given by (22). The maximum diffusivity is predicted to occur when the horizontal scale of events is comparable to the deformation radius ($L \sim R$), and the vertical scales are large enough that events adjust geostrophically. Analysis of dye and microstructure data suggests that for CMO both of these conditions were met.

The scaling results given by (19) and (22) suggest that for CMO the adjustment of mixed patches of fluid may have led to effective lateral diffusivities of $\kappa_H \approx (0.1–10)\ \mathrm{m^2\ s^{-1}}$. These values span the range of the observed lateral dispersion of the dye. Noteworthy, however, is that the dispersion in the first two CMO experiments appears to be underpredicted by (19), whereas the last two experiments are overpredicted by (22); that is, neither scaling alone appears to collapse all the data. Quantitatively, the difference between these scalings is the Ekman number, which depends on both the vertical scale of mixing events h and the background viscosity ν_B. In comparing the predicted dispersion with the CMO results, we have assumed that the Ekman number is of order 10. Furthermore, in all cases, we have assumed that R/L is of order 1. However, if either or both of these nondimensional parameters varied between the first two and last two experiments, this may account for the apparent discrepancy.

Throughout our analysis, we have attempted to keep track of any order-1 constants, provided that they are known [e.g., the factor of 2/3 in (3) and (4), and the factor of 1/2 in our random walk scaling]. The reason for this was to limit the likelihood of many such constants conspiring to give an order of magnitude in our final results. Our final results thus represent our best estimate of the effective lateral dispersion κ_H by this mechanism. Nevertheless, as discussed above, there are still numerous considerations that could modify κ_H either up or down. First, as discussed in section 4b, if mixing events were not horizontally symmetric, geostrophic flows associated with their adjustment may have led to even larger horizontal displacements than suggested by (17). Second, the scaling given by (19) and (22) may underpredict the effective lateral spreading of tracer if the geostrophic flow persists for much longer than an inertial period, since in that case the lateral

advection of the mixed fluid may be larger than the deformation scale. Conversely, as discussed in section 4c, a negative correlation between the step size and frequency in our random walk scaling would imply that (19) overestimates the effective lateral dispersion by this mechanism. Meanwhile, as also discussed in section 2 and 4b, density anomalies observed during the CMO dye studies were frequently oblique rather than parallel to potential density surfaces, which according to (19) would have increased the effective diffusivity due to large events, provided their effective horizontal scale was still not significantly less than R. Last, as discussed in section 4c, if layers do adjust geostrophically and then subsequently decay due to viscous damping, additional spreading of the mixed fluid may occur during the spindown of the geostrophic flow. Again, the effective lateral diffusivity associated with the relaxation of mixing events would thus increase compared to (19).

In conclusion, using our best estimates of the relevant parameters, we believe that stirring by the adjustment of patches of weak stratification resulting from diapycnal mixing events is important to lateral dispersion in the stratified waters of the continental shelf, and perhaps other regions of the ocean. In particular, the predicted dispersion by this mechanism is consistent with the lateral dispersion observed during the CMO dye studies. Despite our best efforts, however, the CMO dye experiments still provide only piecemeal evidence of this mechanism, since the temporal and spatial resolution of the observations were often comparable to or greater than the scales of the mixing events. Compounding the problem is the fact that the velocities associated with the vortical mode are very small, only a few centimeters per second, relative to the ambient internal wave field whose velocities are as high as 40 $\mathrm{cm\,s^{-1}}$ in the CMO region. As a next step, higher-resolution (both temporally and spatially) Lagrangian field studies will be needed to discern the processes acting at these scales in the ocean. Additional dye-release experiments would be particularly useful in this regard because they naturally integrate in both time and space and hence help to filter motions with relatively short time scales from the more persistent, albeit less energetic, vortical motions. Numerical simulations would also be useful as a means of evaluating the parameter dependence proposed here. Both of these are areas of ongoing investigation.

Acknowledgments. The Coastal Mixing and Optics dye studies were funded by the Office of Naval Research under Grants N00014-95-1-0633 (tracer experiments) and N00014-95-1-1063 (AASERT fellowship). Additional analysis was also performed under ONR Grant N00014-01-1-0984. Two anonymous reviewers provided valuable suggestions on earlier drafts of this manuscript.

APPENDIX

Shear Dispersion by Vortical Modes

The scaling arguments of section 3 show that horizontal displacements associated with the adjustment of mixed patches can lead to significant lateral dispersion. A second means of lateral dispersion that can occur during the adjustment of these patches is vertical shear dispersion. Although this mechanism was discussed in detail by SL, the effective shear dispersion due to isolated mixing events was not well represented by their analysis. This is because the relatively low frequency shears associated with these events would have been aliased as high-frequency shears due to the relatively small spatial scales of the events, coupled with the movement of the ship from which the shear was measured.

In our analysis of section 3 we assumed that there is a flow, U, associated with the adjustment of mixing events. Let us now further assume that to lowest order, this flow occurs on the same vertical scale, h, as the mixing event itself. Hence, the adjustment of an event will lead to a vertical shear of order

$$\alpha \sim U/h. \tag{A1}$$

This vertical shear combined with the vertical diffusivity creates the shear dispersion of interest. We now show that the relaxation of diapycnal mixing events leads to shear dispersion that is less than the effective lateral dispersion due to the horizontal displacements associated with such events. To do this, we combine the scaling analysis of section 3 with the results of the shear dispersion analysis of SL.

Assuming a linear shear dispersion model, the effective horizontal diffusivity for an oscillatory shear of amplitude α and frequency ω scales as

$$\kappa_H \sim \frac{\alpha^2}{\omega^2}\kappa_B \tag{A2}$$

(Smith 1982; Young et al. 1982; see also SL). (A background diffusivity κ_B, which acts during the adjustment of a patch, has been introduced here. This background diffusivity will be smaller than κ_z because much of the mixing represented by the latter occurs during the mixing event that creates the patch rather than during the adjustment phase when the shear develops.) Alternatively, for a steady linear shear acting over a time T, the rate of change of tracer variance, that is, the effective horizontal diffusivity, scales as

$$\kappa_H \sim \alpha^2 T^2 \kappa_B \tag{A3}$$

(Smith 1982; see also SL). In this case, the description of the variance in terms of a horizontal diffusivity is not strictly appropriate since the variance grows as the third power of time; however, by writing the horizontal variance in this way, (A2) can be compared directly with

(A3). Specifically, comparison of these expressions shows that for a linear shear, the effective horizontal dispersion by vertical shear dispersion is given by the product of the shear squared, a time scale squared, and the vertical diffusivity. In the case of an oscillatory shear, (A2) shows that the appropriate time scale is given by the period of oscillation. In the case of a mean shear, (A3) shows that the time scale is the duration for which the steady shear persists.

Equation (A3) can be used to estimate the effective lateral dispersion by shear dispersion in the context of the relaxation of diapycnal mixing events. The shear associated with the adjustment (and the ensuing geostrophic flow) can be estimated from (A1). Meanwhile, the duration of the shear can be approximated as the relevant adjustment time scale of events. Last, the velocity scale for the case of geostrophically adjusting mixed layers was given by (16). Combining these results, we obtain

$$\kappa_H \sim \frac{h^2 \Delta N^4}{L^2 f^4} \kappa_B < \left(\frac{N^2}{f^2}\right)\left(\frac{R^2}{L^2}\right)\kappa_z, \qquad \text{(A4)}$$

where we have assumed the time scale $T \sim 1/f$ and the last inequality results since by definition, $\Delta N^2 \leq N^2$, and since $\kappa_B < \kappa_z$. This says that the effective shear dispersion due to the adjustment of diapycnal mixing events is less than the effective horizontal dispersion due to horizontal displacements associated with these same events [i.e., see (19)]. An analogous result can be derived if we consider the effect of the Ekman number on the displacement time scale. In addition, similar results can be obtained for the cases of ageostrophic adjustment. Thus, in general, we find that shear dispersion during the adjustment of the patches scales with the between-event diffusivity in the same way that κ_H due to isopycnal motions scales with the dominant diffusivity; the latter, however, is much larger.

REFERENCES

Alford, M. A., and R. Pinkel, 2000: Observations of overturning in the thermocline: The context of ocean mixing. *J. Phys. Oceanogr.,* **30,** 805–832.

Aref, H., 1983: Integrable, chaotic, and turbulent vortex motion in two-dimensional flows. *Annu. Rev. Fluid Mech.,* **15,** 345–389.

Arneborg, L., 2002: Mixing efficiencies in patchy turbulence. *J. Phys. Oceanogr.,* **32,** 1496–1506.

Garrett, C., and W. Munk, 1972: Oceanic mixing by breaking internal waves. *Deep-Sea Res.,* **19,** 823–832.

Gill, A. E., 1981: Homogeneous intrusions in a rotating stratified fluid. *J. Fluid Mech.,* **103,** 275–295.

Grant, H. L., A. Moilliet, and W. M. Vogel, 1968: Some observations of the occurrence of turbulence in and above the thermocline. *J. Fluid Mech.,* **34,** 443–448.

Gregg, M. C., 1989: Scaling turbulent dissipation in the thermocline. *J. Geophys. Res.,* **94,** 9686–9698.

Griffiths, R. W., and E. J. Hopfinger, 1984: The structure of mesoscale turbulence and horizontal spreading at ocean fronts. *Deep-Sea Res.,* **31,** 245–269.

Henyey, F. S., J. Wright, and S. M. Flatté, 1986: Energy and action flow through the interanal wave field. *J. Geophys. Res.,* **91,** 8487–8495.

Ivey, G. N., 1987: Boundary mixing in a rotating, stratified fluid. *J. Fluid Mech.,* **183,** 25–44.

Kunze, E., 2001: Waves: Vortical mode. *Encyclopedia of Ocean Sciences,* S. T. J. Steele and K. Turekian, Eds., Academic Press, 3174–3178.

Ledwell, J. R., A. J. Watson, and C. S. Law, 1993: Evidence for slow mixing across the pycnocline from an open ocean tracer release experiment. *Nature,* **364,** 701–703.

——, ——, and ——, 1998: Mixing of a tracer in the pycnocline. *J. Geophys. Res.,* **103,** 21 499–21 529.

——, T. F. Duda, M. A. Sundermeyer, and H. E. Seim, 2004: Mixing in a coastal environment. Part I: A view from dye dispersion. *J. Geophys. Res.,* **109**, C10013, doi:10.1029/2003JC002194.

Lin, J. T., and Y. H. Pao, 1979: Wakes in stratified fluids. *Annu. Rev. Fluid Mech.,* **11,** 317–338.

MacKinnon, J. A., and M. C. Gregg, 2003: Mixing on the late-summer New England shelf: Solibores, shear and stratification. *J. Phys. Oceanogr.,* **33,** 1476–1492.

McWilliams, J. C., 1985: Submesoscale, coherent vortices in the ocean. *Rev. Geophys.,* **23,** 165–182.

——, 1988: Vortex generation through balanced adjustment. *J. Phys. Oceanogr.,* **18,** 1178–1192.

Oakey, N. S., 1988: Estimates of mixing inferred from temperature and velocity microstructure. *Small-Scale Turbulence and Mixing in the Ocean: Proceedings of the 19th International Liege Colloquium on Ocean Hydrodynamics*, J. C. J. Nihoul and B. M. Jamart, Eds., Elsevier Oceanography Series, Elsevier Science, 239–247.

——, and B. J. W. Greenan, 2004: Mixing in a coastal environment. Part II: A view from microstructure measurements. *J. Geophys. Res.,* **109** (C10), C10014, doi:10.1029/2003JC002193.

Pasquero, C., A. Provenzale, and A. Babiano, 2001: Parameterization of dispersion in two-dimensional turbulence. *J. Fluid Mech.,* **439,** 279–303.

——, ——, and J. B. Weiss, 2002: Vortex statistics from Eulerian and Lagrangian time series. *Phys. Rev. Lett.,* **89,** 284501, doi:10.1103/PhysRevLett.89.284501.

Phillips, O. M., 1966: *Dynamics of the Upper Ocean.* Cambridge University Press, 261 pp.

Polzin, K. L., and R. Ferrari, 2004: Isopycnal dispersion in NATRE. *J. Phys. Oceanogr.,* **34,** 247–257.

Polzin, K. L., J. M. Toole, and R. W. Schmitt, 1995: Finescale parameterizations of turbulent dissipation. *J. Phys. Oceanogr.,* **25,** 306–328.

——, E. Kunze, J. M. Toole, and R. W. Schmitt, 2003: The partition of finescale energy into internal waves and subinertial motions. *J. Phys. Oceanogr.,* **33,** 234–248.

Provenzale, A., 1999: Transport by coherent barotropic vortices. *Annu. Rev. Fluid Mech.,* **31,** 55–93.

Reznik, G. M., V. Zeitlin, and M. Ben Jelloul, 2001: Nonlinear theory of geostrophic adjustment. Part 1. Rotating shallow-water model. *J. Fluid Mech.,* **445,** 93–120.

Rhines, P. B., 1977: The dynamics of unsteady currents. *The Sea,* E. D. Goldberg et al., Eds., Marine Modeling, Vol. 6, John Wiley and Sons, 189–318.

——, and W. R. Young, 1983: How rapidly is a passive scalar mixed within closed streamlines? *J. Fluid Mech.,* **133,** 133–145.

Smith, R., 1982: Dispersion of tracers in the deep ocean. *J. Fluid Mech.,* **123,** 131–142.

Smyth, W. D., J. N. Moum, and D. R. Caldwell, 2001: The efficiency of mixing in turbulent patches: Inferences from direct simulations and microstructure observations. *J. Phys. Oceanogr.,* **31,** 1969–1992.

Sundermeyer, M. A., 1998: Studies of lateral dispersion in the ocean. Ph.D. thesis, Massachusetts Institute of Technology/

Woods Hole Oceanographic Institution Joint Program, 215 pp.
——, and J. R. Ledwell, 2001: Lateral dispersion over the continental shelf. Analysis of dye-release experiments. *J. Geophys. Res.,* **106,** 9603–9621.
Taylor, G. I., 1921: Diffusion by continuous movements. *Proc. London Math. Soc.,* **20A,** 196–212.
Thomas, P. J., and P. F. Linden, 1996: A laboratory simulations of mixing across tidal fronts. *J. Fluid Mech.,* **309,** 321–344.
Thorpe, S. A., 1999: On internal wave groups. *J. Phys. Oceanogr.,* **29,** 1085–1095.
——, U. Lemmin, C. Perrinjaquet, and I. Fer, 1999: Observations of the thermal structure of a lake using a submarine. *Limnol. Oceanogr.,* **44,** 1575–1582.
Vanneste, J., and P. H. Haynes, 2000: Intermittent mixing in strongly stratified fluids as a random walk. *J. Fluid Mech.,* **411,** 165–185.
Woods, J. D., 1968: Wave-induced shear instability in the summer thermocline. *J. Fluid Mech.,* **32,** 791–800.
——, and R. L. Wiley, 1972: Billow turbulence and ocean microstructure. *Deep-Sea Res.,* **19,** 87–121.
Young, W. R., P. B. Rhines, and C. J. R. Garrett, 1982: Shear-flow dispersion, internal waves and horizontal mixing in the ocean. *J. Phys. Oceanogr.,* **12,** 515–527.